ACS APPLIED MATERIALS & INTERFACES

Research Article

www.acsami.org

Antibody Arrays for Quality Control of Mesenchymal Stem Cells

Ryo Nishikiori, Kotaro Watanabe, and Koichi Kato*

Department of Biomaterials, Institute of Biomedical & Health Sciences, Hiroshima University, 1-2-3 Kasumi, Minami-ku, Hiroshima 734-8553, Japan

Supporting Information

ABSTRACT: Quality control of mesenchymal stem cells is an important step before their clinical use in regenerative therapy. Among various characteristics of mesenchymal stem cells, reproducibility of population compositions should be analyzed according to characteristics, such as stem cell contents and differentiation stages. Such characterization may be possible by assessing the expression of several surface markers. Here we report our attempts to utilize antibody arrays for analyzing surface markers expressed in mesenchymal stem cell populations in a high-throughput manner. Antibody arrays were fabricated using a glass plate on which a micropatterned alkanethiol monolayer was formed. Various antibodies against surface markers including CD11b, CD31, CD44, CD45, CD51, CD73, CD90, CD105, and CD254 were covalently immobilized on the micropatterned surface in an array format to obtain an antibody array. To examine the feasibility of the array, cell binding assays were performed on the array using a mouse mesenchymal stem cell line. Our results showed that cell binding was observed on the arrayed spots with immobilized antibodies which exhibited reactivity to the cells in flow cytometry. It was further found that the density of cells attached to antibody spots was correlated to the mean fluorescent channel recorded in flow cytometry. These results demonstrate that data obtained by cell binding assays on the antibody array are comparable to those by the conventional flow cytometry, while throughput of the analysis is much higher with the antibody array-based method than flow cytometry. Accordingly, we concluded that the antibody array provides a high-throughput analytical method useful for the quality control of mesenchymal stem cells.

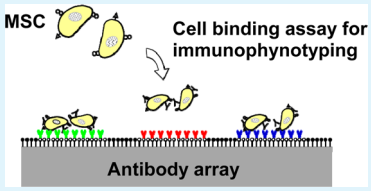

KEYWORDS: *mesenchymal stem cell, patterning, flow cytometry, quality control, antibody*

1. INTRODUCTION

Mesenchymal stem cells (MSCs) are multipotent cell populations obtained from various tissues such as bone marrow, adipose, umbilical cord blood, and dental pulp.[1−4] These cells have a potential to self-renew and differentiate into several tissues of mesenchymal origin.[5,6] Therefore, MSCs are regarded as one of the most promising cell sources for use in regenerative medicine.[7−9] In fact, numerous studies have been made with MSCs for regeneration of various tissues, such as bone, cartilage, and cardiac muscle.[10−13]

Prior to the clinical applications of MSCs for tissue regeneration, we must always consider the quality of the cells that have been processed in vitro.[14,15] For safety reasons, cells are required to be free of infectious pathogens such as viruses, bacteria and parasites. Genetic integrity is another important requisite for transplantation therapy. Besides these criteria, reproducibility of population compositions should be characterized according to characteristics such as stem cell contents and differentiation stages, because MSC populations may contain heterologous cells with respect to their lineages and differentiation stages, and the extent of heterogeneity is a subject of cell sources and culture conditions.

Conventionally population compositions have been analyzed by flow cytometry in which reactivity of antibodies against surface markers is evaluated for individual cells in a population. This method has provided profound possibilities for characterizing living cells used for transplantation. However, throughput of the analysis is still limited even with a state-of-the-art multicolor apparatus. This limitation is critical when analysis is performed for a number of surface markers, as required for the characterization of MSCs for use in transplantation therapy. Therefore, technological advances are absolutely required for a method that allows us to analyze expression of surface markers with much higher throughput. This is highly important for the safe and reproducible treatments through cell transplantation for a number of patients at many clinical facilities.

To address this issue, we have been involved in the development of antibody arrays that provide a novel technique for simply analyzing a pattern of surface marker expression.[16] Antibody arrays are fabricated by displaying different antibodies on a micropatterned, glass-based chip in a site-addressable manner. The expression pattern of surface markers can be attained by inspecting cell adhesion on every antibody spots for assessing simultaneously reactivity of multiple surface antigens with surface-immobilized antibodies. In the present study, we examined the feasibility of antibody arrays for the quantitative characterization of MSC populations with a purpose to establish a practical method for the quality control of MSCs.

2. MATERIALS AND METHODS

2.1. Antibodies and Chemicals. Nine monoclonal antibodies specific for mouse surface antigens were purchased from eBioscience, Inc., San Diego, CA (antibodies for CD11b, CD31, CD45, CD51, CD73, CD90, and CD254), Cedar Lane Laboratories, Burlington,

Received: June 3, 2015
Accepted: July 14, 2015
Published: July 14, 2015

DOI: 10.1021/acsami.5b04860
ACS Appl. Mater. Interfaces 2015, 7, 16828−16836

Ontario, Canada (anti-CD44 antibody), and R&D Systems, Inc., Minneapolis, MN (anti-CD105 antibody). The list of surface markers analyzed in this study and the names of all antibody clones are shown in Table 1.[17,18] The isotype of all antibodies used was IgG class. The

Table 1. List of Surface Markers and Antibody Clones

surface marker	other name [refs 17 and 18]	clone
CD11b	complement receptor 3 (CR3), α_M chain of β_2 integrin	M1/70
CD31	platelet endothelial cell adhesion molecule-1 (PECAM-1)	390
CD44	receptor for hyaluronic acid, phagocytic glycoprotein-1, hermes antigen	KM81
CD45	leukocyte common antigen	30-F11
CD51	α_V subunit of $\alpha_V\beta_3$ integrin	RMV-7
CD73	ecto-5′-nucleotidase	TY/11.8
CD90	Thy-1, theta	G7
CD105	endoglin, receptor for transforming growth factor-β types I and III (TGF-β1 and TGF-β3)	209701
CD254	TNF-related activation-induced cytokine receptor (TRANCE), receptor activator of NF-kappa B ligand (RANKL), osteoprotegerin ligand (OPGL)	IK22/5

freeze-dried powders of antibodies were reconstituted following the manufacturers' instructions, whereas the rest of the antibodies supplied in solution were used as received. The concentration of antibodies was ranged from 0.5 to 1 mg/mL and used without further dilution unless otherwise noted. Rat immunoglobulin G (IgG) was obtained from Sigma Chemical Co., St. Louis, MO and used as control at a concentration of 1 mg/mL in phosphate buffered saline (PBS).

Bovine γ-globulin was obtained from Nacalai Tesque, Inc., Kyoto, Japan. 11-Mercapto-1-undecanoic acid and bovine serum albumin (BSA) were obtained from Sigma. 1-Hexadecanethiol and other chemicals of extra pure grade were purchased from Wako Pure Chemical Industries Ltd., Osaka, Japan, and used without further purification.

2.2. Preparation of Antibody Arrays. Antibody arrays were prepared as before[16] with slight modifications. As shown in Scheme 1, a self-assembled monolayer (SAM) of methyl-terminated 1-hexadecanethiol was formed on a glass plate (24 mm × 24 mm × 0.5 mm) on which a thin gold layer had been deposited by vacuum evaporation. The SAM was then exposed to argon plasma for 30 s using a plasma generator (SEDE/39N, Meiwafosis Co., Ltd., Tokyo, Japan) operated at 10−100 Pa and 6 W through a stainless steel mask (25 mm × 25 mm × 0.5 mm) that had 25 circular holes of 1 mm in diameter, arrayed in 5 × 5 matrix in the center of the mask with an interval of 1 mm between holes. Plasma exposure facilitated decomposition of SAM within irradiated regions. After washing with ethanol, the plate was immersed in ethanol containing 1 mM 11-mercapto-1-undecanoic acid at room temperature for 1 h to form a SAM within irradiated regions to obtain a patterned surface with COOH-terminated hydrophilic, reactive spots arrayed over the CH_3-terminated hydrophobic surroundings. The plate with the patterned SAM was then immersed in *N*,*N*-dimethylformamide (DMF) containing 0.1 M *N*,*N*′-dicyclohexylcarbodiimide (DCC) and 0.05 M *N*-hydroxysuccinimide (NHS) at room temperature for 30 min to activate carboxylic acids present on the spots, and then washed with DMF and acetone. The activated plate was placed on an ice pad to visualize the spots by moisture condensation. Immediately after this procedure, an aliquot of antibody or IgG solutions in PBS (approximately 200 nL each) was manually pipetted onto separate spots on a single plate, and immobilization reaction was allowed to proceed at room temperature for 30 min. Nine antibodies listed in Table 1 were immobilized on a single plate to examine the feasibility of the array for parallel analysis of different surface markers. On the other hand, another type of an antibody array on which only anti-CD105 antibody was immobilized at identical or varying surface densities to study the effect of cell seeding density or the surface density of immobilized antibody. The concentration of antibodies was typically 0.5 or 1 mg/mL, whereas 9.8 × 10^{-4}−1.0 mg/mL anti-CD105 antibody solutions were used to obtain an array that displayed 22 spots with varying densities of antibody and a spot with control IgG. After reaction, the drops of solutions were carefully aspirated, and the plate was immediately immersed in 10% BSA solution in PBS for more than 2 h to block nonspecific cell binding. The antibody array thus obtained was washed with several portions of PBS.

Scheme 1. Preparation of an Antibody Array[a]

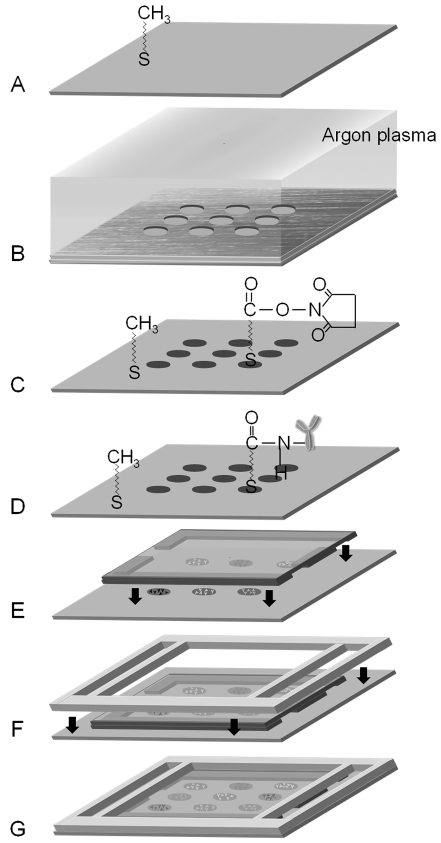

[a](A) A gold-evaporated glass plate with a methyl-terminated SAM. (B) Irradiation of argon plasma through a metal mask to form a patterned surface with bare gold spots. (C) Formation of a carboxylic acid-terminated SAM within the spots and subsequent activation of the terminal carboxylic acid with DCC and NHS. (D) Pipetting antibody solutions to the activated spots to allow for immobilization reaction followed by blocking with albumin. (E) Mounting a cover glass with spacers to create a parallel chamber. (F) Silicone frames were attached to the antibody array to construct a medium reservoir. (G) An antibody array finally assembled.

As previously reported,[19] double adhesive tape (NW-15SF, Nichiban Co., Ltd., Tokyo, Japan) was cut into strips (2.5 mm × 18 mm) and mounted to the both edges of a cover glass (18 mm × 18 mm × 0.15 mm; Matsunami Glass Ind., Ltd., Osaka, Japan) as a spacer (Scheme 1E). The cover glass was adhered to an antibody array in a way that the adhesive tape was inserted as a spacer to create a parallel gap of 240 μm between the array surface and the cover glass. In addition, a sheet of silicone rubber (thickness = 1 mm) was cut into an appropriate shape as shown in Scheme 1F and used to create a medium reservoir to avoid evaporation of a medium during cell binding assays.

2.3. Surface Density of Immobilized Antibody. Because the amount of antibody immobilized on a single spot of an array was too small to be precisely determined, we used a glass plate with immobilized antibody on its entire surface to determine the surface density of antibody immobilized through the coupling reaction as described above. First, a SAM of 11-mercapto-1-undecanoic acid was

DOI: 10.1021/acsami.5b04860
ACS Appl. Mater. Interfaces 2015, 7, 16828−16836

formed directly on the entire surface of a gold-coated glass plate. Then, the terminal carboxylic acids were activated with a combination of DCC and NHS followed by coupling of rat IgG using solutions with different concentrations (3−1000 μg/mL) in a similar fashion as described above. Subsequently the plate was extensively washed with PBS to remove unreacted IgG. The surface density of immobilized IgG was determined using a microBCA protein assay kit (Thermo Scientific, Waltham, MA): A silicone frame having a square window (area = ∼5 cm^2) was placed on the IgG-immobilized surface. MicroBCA reaction mixture (400 μL) was pipetted within the window, and the temperature was kept at 37 °C for 3 h to allow coloring reaction. The absorbance at 562 nm was measured for the resultant solution using a spectrophotometer (Varioskan Flash, Thermo Scientific, Waltham, MA). The amount of immobilized IgG was determined using BSA as a standard.

For detecting antibodies immobilized to a single spot on an array, we further employed immunological staining. An array with immobilized nine antibodies listed in Table 1 and control IgG (without a parallel chamber setup) was immersed in PBS containing 50% Blocking One reagent (Nacalai Tesque, Inc.) and 0.025% Tween-20 (PBS-BT) to block nonspecific adsorption of secondary antibody. After incubation for 1 h, the solution was carefully aspirated, and the surface was exposed to PBS-BT containing 10 μg/mL goat antirat IgG antibody conjugated with Alexa Fluor 488 (Invitrogen, Carlsbad, CA) and incubated for 30 min at room temperature. After washing with PBS-BT, the array was observed with a fluorescence microscope (IX73, Olympus Corp., Tokyo, Japan). Fluorescent intensity was determined for four quadrate areas (0.2 mm × 0.2 mm each) on an antibody spot using ImageJ software (NIH, Bethesda, MD) and averaged.

2.4. Cell Culture. A murine mesenchymal stem cell line (C3H10T1/2) and an osteoblast-like cell line derived from mouse calvarias (MC3T3-E1) were obtained from Riken BioResource Center, Ibaraki, Japan. These cells were cultured in Dulbecco's modified medium (Sigma) supplemented with 10% fetal bovine serum (FBS; Biological Industries, Ltd., Kibbutz Beit-Haemek, Israel), 100 U/mL penicillin (Sigma), and 0.1 mg/mL streptomycin (Sigma) at 37 °C under 5% CO_2 atmosphere.

2.5. Cell Binding Assay. C3H10T1/2 cells were harvested by treatment with Accutase (Innovative Cell Technologies, Inc., San Diego, CA) at room temperature. The cells were suspended in an acridine orange (AO) solution (1 μg/mL) for 15 min to stain their nuclei and washed twice with PBS containing 2% FBS. Subsequently the cells were suspended at typically 5.0 × 10^6 cells/mL in PBS containing 1 mg/mL bovine γ-globulin and 0.53 mM *N,N,N′,N′*-ethylenediaminetetraacetic acid (EDTA) and incubated at room temperature for 10 min to block receptors for the fragment crystallizable (Fc) of immunoglobulin. The cell suspension (70 μL) was gently infused into an antibody array through the inlet (Scheme 1G). With a suspension at 5.0 × 10^6 cells/mL, cell density reached 1200 cells per square millimeter. On the other hand, when the effect of seeding density was studied, suspensions at varying cell concentrations (1.0 × 10^6−2.0 × 10^7 cells/mL for a seeding density of 150−3600 cells/mm^2) were used. The infused cells were incubated in an antibody array for 15 min at 37 °C under 5% CO_2 atmosphere to effect cell binding to the spots with reactive antibodies. After 15 min, the array was gently inverted, so that unbound cells were detached from the array surface by their own gravity to come down to the bottom face (the cover glass side), leaving bound cells underneath the array surface.[19] The inverted array was mounted on the fluorescent microscope (IX73, Olympus Corp., Tokyo, Japan), and the bound cells were visualized by adjusting a focus plane in close proximity to the array surface. In fluorescent imaging, cells bound to an antibody spot were in focus, visualized with a clear outline at their peripheral regions of an AO-stained nucleus. On the other hand, thanks to the nonfouling coating of albumin, cells that have no reactivity to the immobilized antibody came down to the cover glass side upon inversion of the array. Because there is a 0.24 mm-gap between the array surface and the cover glass, the nonbound cells at the cover glass side were out of focus, visualized just as broad background, when adhering cells are observed with a microscope. Thus, adhering cells were easily distinguished from nonadhering cells, and the number of cells adhering to a spot could be determined by counting cells on a fluorescent image.

In order to examine the feasibility of detecting small deviation in the fraction of specific cells, further study was carried out using physical mixtures of C3H10T1/2 (mesenchymal stem cells) and MC3T3-E1 (as a model for the cells that are slightly committed to an osteoblast lineage) cells. C3H10T1/2 cells previously stained with AO were mixed with nonstained MC3T3-E1 at various mixing ratios, while total cell concentrations were kept constant at 5 × 10^6 cells/mL. The mixed cell suspensions were injected to the array that displayed anti-CD105 antibody and control IgG. The density of total cells (C3H10T1/2 plus MC3T3-E1) bound to an anti-CD105 antibody spot was determined from a phase-contrast image, while a fluorescent image was used to count fluorescently active C3H10T1/2 cells.

2.6. Flow Cytometry. Flow cytometry was performed according to the standard procedures.[20] In brief, after blocking of Fc receptors with PBS containing 2% FBS (washing medium), C3H10T1/2 and MC3T3-E1 cells were reacted with antibodies listed in Table 1, followed by reaction with goat antirat IgG antibody conjugated with Alexa Fluor 488. The cells were analyzed with FACSCalibur flow cytometer (Becton Dickinson, New Jersey, USA). Twenty thousand events were acquired to draw a histogram, determining the mean channel fluorescence. Control experiments were performed using a reference population reacted with control IgG instead of specific antibodies, followed by exposure to Alexa Fluor 488-conjugated antirat IgG.

3. RESULTS

3.1. Preparation of Antibody Arrays. In this study, antibody arrays were fabricated in a fashion similar to that reported previously.[16] For creating a pattern of alkanethiol monolayers, however, plasma irradiation was employed in the present study instead of photo irradiation as we did in the previous study. A methyl-terminated SAM was treated here with 10 mA plasma for 30 s, whereas in the previous study a SAM was treated with light from a 500 W mercury lamp for 2 h. We found that both methods gave similar results, but plasma irradiation greatly facilitated to save time for the fabrication of antibody arrays.

After activation of terminal carboxylic acids within every spots on the patterned SAM, antibodies were covalently immobilized. Immobilization reaction was confirmed by immunofluorescent staining of the antibodies using goat antirat IgG antibody conjugated with an Alexa 488 fluorophore. As shown in Figure 1A, all the dots were stained in green fluorescence. Fluorescence intensity (Figure 1B) was significantly higher than background in all cases, although the intensities varied depending on antibodies used for immobilization reaction. The variation seen in the fluorescent intensity (Figure 1B) seems to be due to a difference in immobilized antibodies. However, the reproducibility was not a significant problem when the same antibody clone was always used, as evidenced by the small error bars that show the reproducibility for each case. In addition, some spots had the contour which did not exactly replicate the circular shape of the mask, most likely due to inaccuracy in manual pipetting of antibody solutions.

Because the amount of antibody immobilized on a single spot was too small to determine, quantitative analysis was conducted for IgG immobilized on the entire surface of a glass plate through the same chemistry as for antibody arrays. Figure 2 shows the amount of IgG immobilized onto the glass surface as a function of IgG concentrations in the solution used for the

DOI: 10.1021/acsami.5b04860
ACS Appl. Mater. Interfaces 2015, 7, 16828−16836

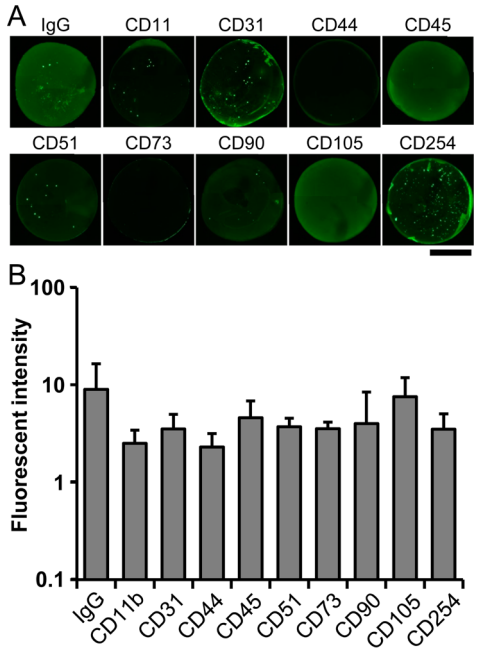

Figure 1. Immobilization of antibodies on a micropatterned plate. (A) Fluorescent images of the spots on a single plate. Nine different antibodies were immobilized on separate spots. Antibodies were visualized with Alexa Fluor 488-conjugated anti-IgG antibody. Scale bar = 500 μm. (B) Fluorescence intensity measured for every spots with immobilized antibodies. Data are expressed as the mean for two independent plates. The data are expressed as the mean ± standard deviation for n = 5.

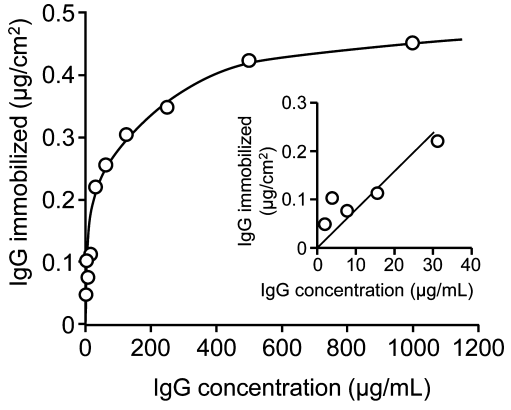

Figure 2. Density of IgG immobilized onto the surface of a carboxylic acid-terminated SAM. An inset shows a curve for low IgG concentration.

reaction. As can be seen in the inset, the curve exhibited a linear increase at low IgG concentration. At higher IgG concentration, the amount of immobilized IgG gradually increased with its concentration and reached approximately 0.45 μg/cm^2. In the later experiments, we used antibody solutions of 0.5 or 1 mg/mL for antibody array preparation.

3.2. Flow Cytometry. Figure 3 shows histograms obtained from flow cytometry analyses of C3H10T1/2 cells using antibody clones listed in Table 1. It can be seen that the cells were reactive for antibodies to CD44, CD51, CD90 and CD105, but not for those against CD11b, CD31, CD45, and CD254. The histogram for CD90 split into two phases, indicating the presence of two populations with low and high levels of CD90 expression. However, we can assume from the comparison with the control histogram that C3H10T1/2 cells expressed CD90. These results are in good agreement with previous reports on the surface markers of MSCs.[21−24] On the other hand, no reactivity was observed for anti-CD73 antibody, though CD73 was reported to be expressed on human MSCs.[25,26] This discrepancy observed for CD73 is probably ascribed to the difference in an origin of the cells. Accordingly, we can summarize that C3H10T1/2 cells express CD44, CD51, CD90, and CD105, but not CD11b, CD31, CD45, CD73, and CD254.

On the other hand, flow cytometry analysis (Supporting Information Figure S1) showed that no CD105 was expressed on MC3T3-E1 cells used for comparison in later experiments.

3.3. Cell Binding Assays on Antibody Arrays. Cell binding assays were carried out on an array having 10 spots onto which antibodies to CD11b, CD31, CD44, CD45, CD51, CD73 CD90, CD105, and CD254 and control IgG were immobilized.

In preliminary experiments, C3H10T1/2 cells were harvested from tissue culture polystyrene dishes in four different manners: mechanical scraping, EDTA treatment followed by pipetting, trypsinization and treatment with Accutase. All these methods gave similar results in cell binding assays. However, Accutase treatment turned out to be most appropriate because this treatment caused relatively minor damage of cells and rarely yielded cell aggregates. Therefore, we adopted Accutase treatment for later experiments.

The suspension of AO-stained C3H10T1/2 cells was injected into the antibody array to allow for cell binding. The array was gently inverted 15 min after injection to remove unbound cells, and bound cells were observed with a fluorescent microscope. As shown in Figure 4, cells are seen as bright dots on the spots with immobilized antibody to CD44, CD51, CD90, and CD105, but not to CD11b, CD31, CD45, CD73, and CD254. Dim fluorescence observed in all micrographs (example, an area surrounding the anti-CD105 antibody spot) was from unbound cells submerged to the cover glass side in an inverted array. The bound and unbound cells could be easily distinguished by adjusting a focal plane to the vicinity of an array surface under a fluorescent microscope. As described above, anti-CD44, -CD51, -CD90, and -CD105 antibodies were reactive in flow cytometry, while anti-CD11b, -CD31, -CD45, -CD73, and -CD254 antibodies and control IgG showed no reactivity to C3H10T1/2 cells. These agreements between flow cytometry and binding assays on the array suggest that the observed cell adhesion to particular antibody spots is based on the expression of the respective surface antigens.

Cell binding assays were further carried out on an array having nine spots onto all of which anti-CD105 antibody was immobilized under identical conditions for every spots. The suspensions of different cell concentrations were used in binding assays to examine the effect of seeding density. As shown in Figure 5A, bound cells were seen as bright and clear dots within circular antibody spots. The density of bound cells was determined and plotted as a function of seeding density in Figure 5B. As can be seen, bound cell density linearly increased with an increase in seeding density up to 2400 cells/mm^2 and reached constant at higher seeding densities.

In other experiments we used an antibody array having 23 spots onto which anti-CD105 antibody was immobilized from solutions of different antibody concentrations. Cell binding assays were performed at the seeding density of 1200 cells/

DOI: 10.1021/acsami.5b04860
ACS Appl. Mater. Interfaces 2015, 7, 16828−16836

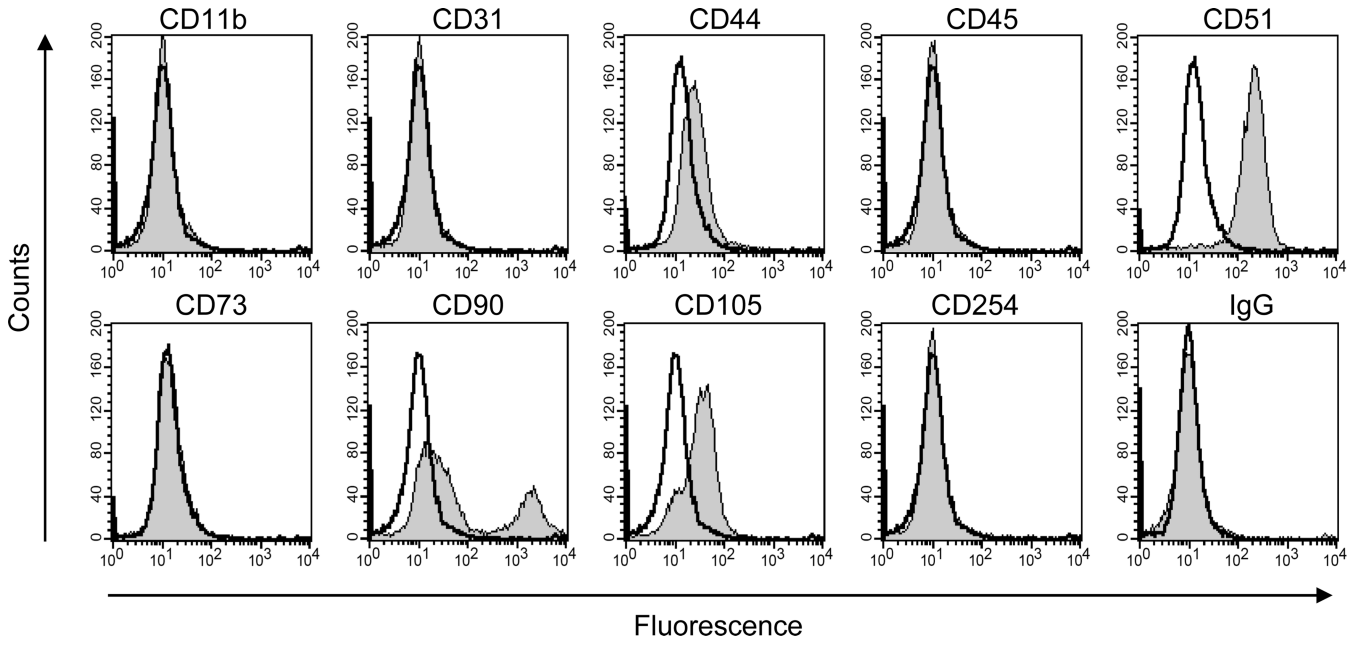

Figure 3. Results of flow cytometry for C3H10T1/2 cells. Shaded curves represent histograms for cells treated with one of the primary antibodies and a fluorescently active secondary antibody. Open curves represent the result of a control experiment in which IgG was used instead of primary antibodies.

mm^2. As shown in Figure 6, the density of bound cells increased linearly with an increase in antibody concentration in the range below 125 μg/mL and reached 1191 ± 32 cells/cm^2. At a concentration more than 125 μg/mL a constant density of bound cells was observed.

3.4. Comparison between Assays with Antibody Arrays and Flow Cytometry. Cell binding assays were performed using arrays on which 9 antibodies and control IgG were displayed, and the density of bound cells were determined for every antibody spots. On the other hand, mean channel fluorescent intensities observed in flow cytometry analyses were determined as representative measures for antibody reactivity, and thus expression of surface antigens. These results are shown in Table 2. The data obtained from cell binding assays on antibody arrays cannot be directly compared with that from flow cytometry, because these data represent different aspects of antibody reactivity to surface markers. However, it may be possible to correlate these two data by scoring them according to the bound cell density and fluorescence intensity, respectively. As shown in Table 2, it is obvious that the scores for a bound cell density are in good agreement with those for a fluorescence intensity in flow cytometry, indicating that these two methods provide comparable information on the expression of surface markers.

3.5. Quantitative Assessment of MSCs. To examine the feasibility of an antibody array to quantitatively detect variations in MSC contents, mixed suspensions containing C3H10T1/2 and MC3T3-E1 at various mixing rations were used in cell binding assays on the arrays that displayed anti-CD105 antibody (3 spots) and control IgG (3 spots). As shown by the flow cytometry analyses (Figure 3 and Supporting Information Figure S1), CD105 antigen is expressed on C3H10T1/2 cells but not MC3T3-E1 cells. In this experiment, C3H10T1/2 cells were stained with a fluorescently active AO dye and mixed with unstained MC3T3-E1 cells. From the comparison of a phase-contrast image (total cells could be imaged) with a fluorescent image (only C3H10T1/2 cells could be imaged), more than 99% of bound cells were identified as C3H10T1/2 cells with very little number of nonspecifically adsorbed MC3T3-E1 cells (These images are shown in Supporting Information Figure S2). As shown in Figure 7, the density of bound cells on anti-CD105 antibody spots, hence C3H10T1/2 cells, increased in proportion to the content of C3H10T1/2 cells in suspension in the entire range of mixing ratios with a high correlation coefficient of linear approximation (R^2 = 0.9942), while negligible numbers of cells were observed on control IgG spots at any osteoblast contents in suspension.

4. DISCUSSION

Every products of MSCs must be thoroughly inspected before their clinical applications. Among various characteristics of MSCs processed in vitro, reproducibility in product composition is one of the most important aspects for safe and standardized treatments using MSCs. In this study, we focused on the expression of surface markers as a trait that specifies populations of MSCs, demonstrating the feasibility of antibody arrays for analyzing the pattern of surface markers expressed on MSCs in a high-throughput manner.

In our previous study,[19,27] we demonstrated that antibody arrays could be successfully used for immunophynotyping of leukemia cells. Antibody arrays were also tested using neural stem cells[16] and an immortalized human MSC line to demonstrate their feasibility for analyzing adherent cells.[27] On the basis of these previous studies, we prepared here antibody arrays through the similar scheme (Scheme 1) as before, while spotting a panel of antibodies newly selected especially for MSCs (Table 1).

The selection of an antibody panel was based on our idea that several antibodies specific for MSCs should be contained in the panel. In addition, the panel should contain other antibodies potentially interact with surface antigens expressed on non-MSCs such as cells of hematopoietic and osteoblastic lineages for assessing concomitantly contained non-MSCs. Therefore, a panel of antibodies immobilized on an array was

DOI: 10.1021/acsami.5b04860
ACS Appl. Mater. Interfaces 2015, 7, 16828−16836

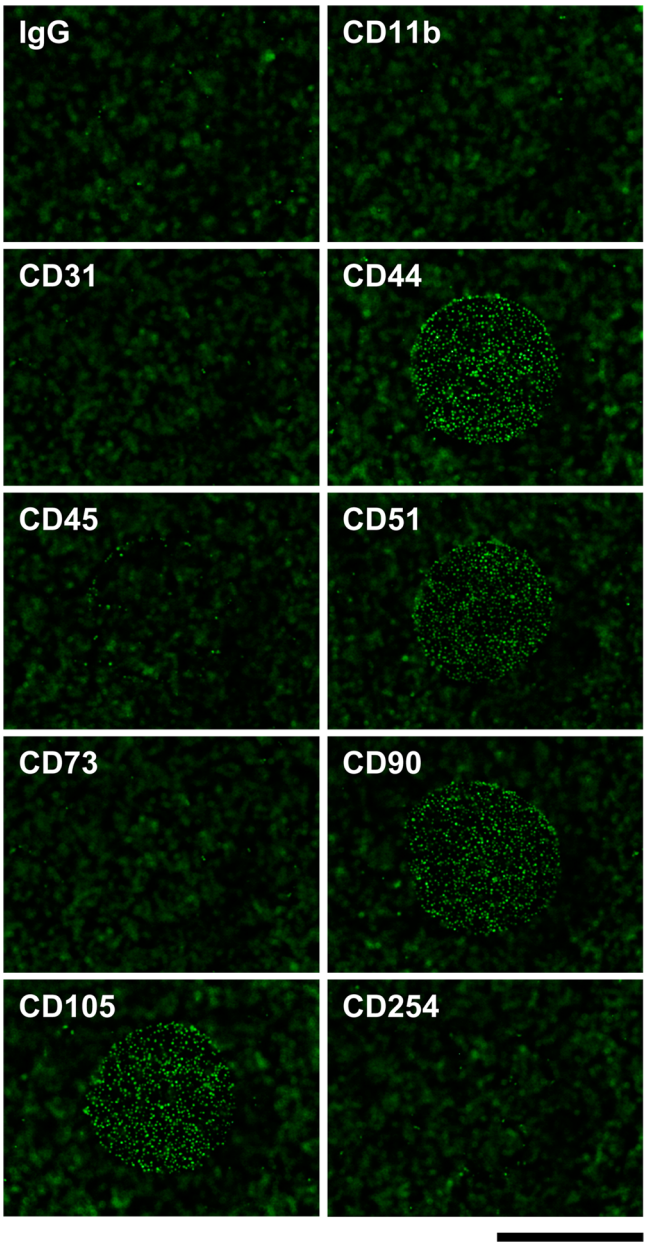

Figure 4. Fluorescent images of AO-stained C3H10T1/2 cells bound to the antibody array that displayed 9 different antibodies and control IgG. The identification of the spots are shown in each photograph. Scale bar: 1 mm.

mainly selected according to the minimal criteria reported by the International Society for Cellular Therapy (ISCT),[28] together with other information previously reported.[29−31] However, it seems that the validity of the antibody panel should be reconsidered depending on the conditions of cell processing such as source of cells and probable concomitance of cells in other lineages. Moreover, as stated by the ISCT, the panel of MSC-specific surface antigens will probably be revised based on future research.

One of the major findings of this study is that, as demonstrated in Figure 7, the density of cells bound to the specific antibody spots is proportional to the content of these cells in suspension. This denotes that the antibody arrays enable us to quantitatively assess the content of specific cells present in MSC populations.

The capability of quantitative detection suggests the mechanism that total cells injected into the chamber first sediment onto the surface of an antibody array while keeping its composition. Then, the cells that express a surface marker specific for the immobilized antibody are captured on the surface through the antigen−antibody interaction, whereas other cells with no surface marker are just kept stationary on the array. Upon inversion of the antibody array, it is likely that cells binding to immobilized antibody are exclusively left bound on the array, while other cells with no binding detach from the array by their own gravity to sediment to the other side. It can be assumed that the composition of a cell at surface does not considerably change during these processes. Accordingly it is able to determine the content of specific cells in suspension from the density of bound cells divided by the seeding density.

Importantly, translational dislocation of cells on the arrays would cause enrichment of the specific cells, overestimating the content of the cells in suspension. In deed, our results suggest that this is not the case. Such dislocation might be significantly suppressed by the parallel chamber configuration as well as the method in which the array is gently inverted to eliminate unbound cells.

The surface density of immobilized antibody may have an impact on the capacity of cell binding. To address this issue, we examined cell binding to the spots on which anti-CD105 antibody was immobilized at different densities. Our results showed that the number of bound cells linearly increased with an increase in antibody concentration up to 125 μg/mL (Figure 6). Beyond this concentration, bound cell number was constant at a density that as similar to the seeding density. These results indicate that antibody solution at more than 125 μg/mL is high enough to totally capture CD105-expressing cells on the antibody spot.

Another factor that would have an influence on bound cell numbers includes the density of seeded cells. As shown in Figure 5, seeding at more than 2000 cells/mm^2 resulted in the constant number of bound cells, most likely because 2000 cells/mm^2 goes above the density for monolayer formation. In the case of excess seeding, only the bottom cells in a multilayer have a direct interaction with immobilized antibody, whereas cells in the upper layers having no contact with immobilized antibody cannot be captured even though these cells express the specific antigen. Therefore, to determine the content of specific cells in suspension, it is necessary that the density of bound cells is divided by the seeding density when cells were seeded at less than 2000 cells/mm^2, but divided by constant 2000 cells/mm^2 when cells were seeded at more than 2000 cells/mm^2.

It was further demonstrated that the data obtained by cell binding assays on the antibody array was fairly comparable with those obtained by flow cytometry as demonstrated in Table 2. This finding provides the proof of principle for the feasibility of the antibody array as an alternative tool for the characterization of MSC populations. In the case of CD90, we observed two peaks in flow cytometry analysis. This result indicates the presence of two populations, CD90^{low} and CD90^{high}, that have different reactivities for the antibody used. Such a result is not peculiar because a similar result was also reported for this cell line even with an antibody clone different from ours.[32] Because the CD90^{low} population also express the surface antigen and can be recognized by the antibody, it can be expected that total cells are captured at the surface with immobilized anti-CD90

DOI: 10.1021/acsami.5b04860
ACS Appl. Mater. Interfaces 2015, 7, 16828−16836

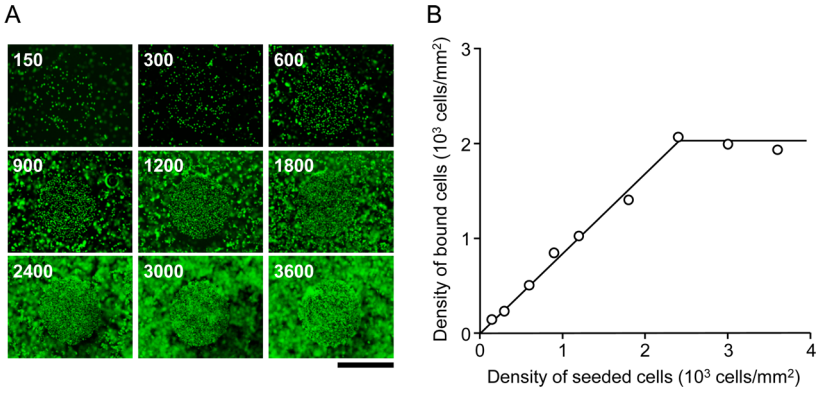

Figure 5. Relationship between cell seeding density and the density of bound cells. (A) Fluorescent images of AO-stained C3H10T1/2 cells bound to the spots with anti-CD105 antibody. Numbers shown in each photograph represent the density of seeded cells in cells/mm^2. Scale bar: 1 mm. (B) The number of C3H10T1/2 cells bound to an anti-CD105 antibody spot as a function of seeding density. Data are expressed as the mean ± standard deviation for n = 4.

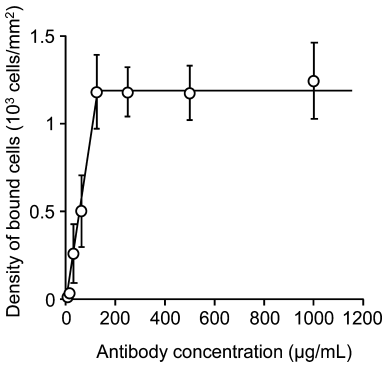

Figure 6. Relationship between the amount of immobilized anti-CD105 antibody and the number of bound C3H10T1/2 cells. Cells were seeded at 1200 cells/mm^2. The data are expressed as the mean ± standard deviation for n = 3–6.

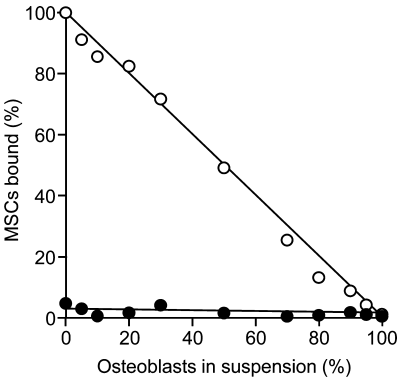

Figure 7. Binding of C3H10T1/2 cells (MSCs) out of mixed suspensions of C3H10T1/2 and MC3T3-E1 cells (osteoblasts) at various mixing ratios to the spot with (open circle) anti-CD105 antibody and (closed circle) control IgG.

Table 2. Results of Immunophenotyping by Antibody Array-Based Cytometry and Flow Cytometry (FCM)

surface marker	density of bound cells on antibody array (cells/mm^2)[a]	score based on cell density[b]	mean fluorescence intensity determined by FCM	score based on peak channel[b]
CD11b	23 ± 18	−	15.8	−
CD31	9 ± 10	−	17.2	−
CD44	671 ± 200	++	67.0	++
CD45	81 ± 64	−	20.6	−
CD51	1106 ± 162	++	268.1	++
CD73	19 ± 18	−	19.3	−
CD90	1030 ± 348	++	483.0	++
CD105	1108 ± 109	++	39.0	++
CD254	1 ± 2	−	28.0	−
IgG (control)	11 ± 13	−	22.6	−

[a]The data are expressed as mean ± standard deviation for n = 3. [b]Score: − low, + moderate, ++ high.

antibody, as evidenced by our results (Table 2), showing no effect on assay specificity.

Importantly, antibody arrays provide a high-throughput method that enable us with analyzing the expression of multiple surface markers at once. This is not always straightforward by flow cytometry even if the latest multicolor flow cytometer is used, although simultaneous expression of multiple markers on an identical cell can be analyzed by flow cytometry. Besides this, compare to flow cytometry, the antibody array-based method has several advantages: Analysis can be performed using smaller number of cells per surface marker and does not require analysts' proficiency in data interpretation as well as an expensive cytometer. To increase the throughput of analysis, it may be practical to automate some of the analytical process such as determination of bound cell densities.[19] All these advantages over flow cytometry highlight the usefulness of the antibody array-based method conceivably for routine analyses.

5. CONCLUSIONS

This study demonstrated that surface antibodies expressed in MSC populations can be analyzed by simple cell binding assays on the antibody array fabricated using the properly designed panel of antigens. The density of cells bound to antibody spots provides a quantitative measure with regard to the composition of cells that express specific surface markers. The data obtained by binding assays on the antibody arrays are comparable to those by conventional flow cytometry. Importantly, the throughput of an analysis is much higher with the antibody array-based method than flow cytometry. Therefore, it may be concluded that the antibody array can be a versatile tool for the quality control of MSCs.

DOI: 10.1021/acsami.5b04860
ACS Appl. Mater. Interfaces 2015, 7, 16828–16836

■ ASSOCIATED CONTENT

Supporting Information

Result of flow cytometry analysis for the expression of CD105 on MC3T3-E1 cells and phase-contrast and fluorescent images of cells bound to an identical spot with immobilized anti-CD105 antibody. The Supporting Information is available free of charge on the ACS Publications website at DOI: 10.1021/acsami.5b04860.

■ AUTHOR INFORMATION

Corresponding Author

*E-mail kokato@hiroshima-u.ac.jp. Phone: +81-82-257-5645. Fax: +81-82-257-5649.

Author Contributions

The manuscript was written through contributions of all authors. All authors have given approval to the final version of the manuscript.

Notes

The authors declare no competing financial interest.

■ ACKNOWLEDGMENTS

This study was supported by Adaptable and Seamless Technology Transfer Program through Target-driven R&D, Japan Science and Technology Agency (AS231Z04602F) and Grant-in-Aid for Scientific Research, Ministry of Education, Culture, Sports, Science and Technology (25670832).

■ REFERENCES

(1) Pittenger, M. F.; Mackay, A. M.; Beck, S. C.; Jaiswal, R. K.; Douglas, R.; Mosca, J. D.; Moorman, M. A.; Simonetti, D. W.; Craig, S.; Marshak, D. R. Multilineage Potential of Adult Human Mesenchymal Stem Cells. *Science* **1999**, *284*, 143−147.

(2) Zuk, P. A.; Zhu, M.; Mizuno, H.; Huang, J.; Futrell, J. W.; Katz, A. J.; Benhaim, P.; Lorenz, H. P.; Hedrick, M. H. Multilineage Cells from Human Adipose Tissue: Implications for Cell-Based Therapies. *Tissue Eng.* **2001**, *7*, 211−228.

(3) Wang, H. S.; Hung, S. C.; Peng, S. T.; Huang, C. C.; Wei, H. M.; Guo, Y. J.; Fu, Y. S.; Lai, M. C.; Chen, C. C. Mesenchymal Stem Cells in the Wharton's Jelly of the Human Umbilical Cord. *Stem Cells* **2004**, *22*, 1330−1337.

(4) Zhang, W.; Walboomers, X. F.; Shi, S.; Fan, M.; Jansen, J. A. Multilineage Differentiation Potential of Stem Cells Derived from Human Dental Pulp after Cryopreservation. *Tissue Eng.* **2006**, *12*, 2813−2823.

(5) Uccelli, A.; Moretta, L.; Pistoia, V. Mesenchymal Stem Cells in Health and Disease. *Nat. Rev. Immunol.* **2008**, *8*, 726−736.

(6) Fong, C. Y.; Chak, L. L.; Biswas, A.; Tan, J. H.; Gauthaman, K.; Chan, W. K.; Bongso, A. Human Wharton's Jelly Stem Cells Have Unique Transcriptome Profiles Compared to Human Embryonic Stem Cells and Other Mesenchymal Stem Cells. *Stem Cell Rev.* **2011**, *7*, 1−16.

(7) Harris, D. T. Umbilical Cord Tissue Mesenchymal Stem Cells: Characterization and Clinical Applications. *Curr. Stem Cell Res. Ther.* **2013**, *8*, 394−399.

(8) Hynes, K.; Menicanin, D.; Han, J.; Marino, V.; Mrozik, K.; Gronthos, S.; Bartold, P. M. Mesenchymal Stem Cells from iPS Cells Facilitate Periodontal Regeneration. *J. Dent. Res.* **2013**, *92*, 833−839.

(9) Toguchida, J. Regenerative Medicine for Bone Diseases Using Mesenchymal Stem Cells. *Inflammation Regener.* **2013**, *33*, 48−53.

(10) Sensebé, L.; Krampera, M.; Schrezenmeier, H.; Bourin, P.; Giordano, R. Mesenchymal Stem Cells for Clinical Application. *Vox Sang.* **2010**, *98*, 93−107.

(11) Kaveh, K.; Ibrahim, R.; Bakar, M. A. Z.; Ibrahim, T. A. Mesenchymal Stem Cells, Osteogenic Lineage and Bone Tissue Engineering: A Review. *J. Anim. Vet. Adv.* **2011**, *10*, 2317−2330.

(12) Le Blanc, K.; Ringdén, O. Mesenchymal Stem Cells: Properties and Role in Clinical Bone Marrow Transplantation. *Curr. Opin. Immunol.* **2006**, *18*, 586−591.

(13) Giordano, A.; Galderisi, U.; Marino, I. R. From the Laboratory Bench to the Patient's Bedside: An Update on Clinical Trials with Mesenchymal Stem Cells. *J. Cell. Physiol.* **2007**, *211*, 27−35.

(14) Sensebé, L. Clinical Grade Production of Mesenchymal Stem Cells. *Biomed. Mater. Eng.* **2008**, *18*, S3−10.

(15) Sensebé, L.; Bourin, P. Mesenchymal Stem Cells for Therapeutic Purposes. *Transplantation* **2009**, *87*, S49−53.

(16) Ko, I.-K.; Kato, K.; Iwata, H. Parallel Analysis of Multiple Surface Markers Expressed on Rat Neural Stem Cells Using Antibody Microarrays. *Biomaterials* **2005**, *26*, 4882−4891.

(17) Kipps, T. J. The Cluster of Differentiation Antigens. In *Williams Hematology*, 6th ed.; Beutler, E., Lichtman, M. A., Coller, B. S., Kipps, T. J., Seligsohn. U., Eds.; McGraw-Hill: New York, 2000; 141−152.

(18) Kamijo, S.; Nakajima, A.; Ikeda, K.; Aoki, K.; Ohya, K.; Akiba, H.; Yagita, H.; Okumura, K. Amelioration of Bone Loss in Collagen-induced Arthritis by Neutralizing Anti-RANKL Monoclonal Antibody. *Biochem. Biophys. Res. Commun.* **2006**, *347*, 124−132.

(19) Kato, K.; Ishimuro, T.; Arima, Y.; Hirata, I.; Iwata, H. High-throughput Immunophenotyping by Surface Plasmon Resonance Imaging. *Anal. Chem.* **2007**, *79*, 8616−8623.

(20) Loken, M. R.; Green, C. L.; Wells, D. A. Immunofluorescence of Surface Markers. In *Flow Cytometry*, 3rd ed.; Ormerod, M. G., Ed.; Oxford University Press: Oxford, U.K., 2000; pp 61−82.

(21) Tran, H. L. B.; Doan, V. N.; Le, H. T.; Ngo, L. T. Various Methods for Isolation of Multipotent Human Periodontal Ligament Cells for Regenerative Medicine. *In Vitro Cell. Dev. Biol.: Anim.* **2014**, *50*, 597−602.

(22) Seeberger, K. L.; Dufour, J. M.; Shapiro, A. M.; Lakey, J. R.; Rajotte, R. V.; Korbutt, G. S. Expansion of Mesenchymal Stem Cells from Human Pancreatic Ductal Epithelium. *Lab. Invest.* **2006**, *86*, 141−153.

(23) Montanucci, P.; Basta, G.; Pescara, T.; Pennoni, I.; Di Giovanni, F.; Calafiore, R. New Simple and Rapid Method for Purification of Mesenchymal Stem Cells from the Human Umbilical Cord Wharton Jelly. *Tissue Eng., Part A* **2011**, *17*, 2651−2661.

(24) Wang, H. S.; Hung, S. C.; Peng, S. T.; Huang, C. C.; Wei, H. M.; Guo, Y. J.; Fu, Y. S.; Lai, M. C.; Chen, C. C. Mesenchymal Stem Cells in the Wharton's Jelly of the Human Umbilical Cord. *Stem Cells* **2004**, *22*, 1330−1337.

(25) Morgan, J. T.; Wood, J. A.; Walker, N. J.; Raghunathan, V. K.; Borjesson, D. L.; Murphy, C. J.; Russell, P. Human Trabecular Meshwork Cells Exhibit Several Characteristics of, But Are Distinct from, Adipose-derived Mesenchymal Stem Cells. *J. Ocul. Pharmacol. Ther.* **2014**, *30*, 254−266.

(26) Marrelli, M.; Paduano, F.; Tatullo, M. Cells Isolated from Human Periapical Cysts Express Mesenchymal Stem Cell-like Properties. *Int. J. Biol. Sci.* **2013**, *9*, 1070−1078.

(27) Kato, K.; Toda, M.; Iwata, H. Antibody Arrays for Quantitative Immunophenotyping. *Biomaterials* **2007**, *28*, 1289−1297.

(28) Dominici, M.; Le Blanc, K.; Mueller, I.; Slaper-Cortenbach, I.; Marini, F.; Krause, D.; Deans, R.; Keating, A.; Prockop, Dj.; Horwitz, E. Minimal Criteria for Defining Multipotent Mesenchymal Stromal Cells. The International Society for Cellular Therapy Position Statement. *Cytotherapy* **2006**, *8*, 315−317.

(29) Díaz-Prado, S.; Muiños-López, E.; Hermida-Gómez, T.; Rendal-Vázquez, M. E.; Fuentes-Boquete, I.; de Toro, F. J.; Blanco, F. J. Multilineage Differentiation Potential of Cells Isolated from the Human Amniotic Membrane. *J. Cell. Biochem.* **2010**, *111*, 846−857.

(30) Arufe, M. C.; De la Fuente, A.; Fuentes, I.; de Toro, F. J.; Blanco, F. J. Chondrogenic Potential of Subpopulations of Cells Expressing Mesenchymal Stem Cell Markers Derived from Human Synovial Membranes. *J. Cell. Biochem.* **2010**, *111*, 834−845.

(31) Pasquinelli, G.; Pacilli, A.; Alviano, F.; Foroni, L.; Ricci, F.; Valente, S.; Orrico, C.; Lanzoni, G.; Buzzi, M.; Luigi Tazzari, P.; Pagliaro, P.; Stella, A.; Paolo Bagnara, G. Multidistrict Human

DOI: 10.1021/acsami.5b04860
ACS Appl. Mater. Interfaces 2015, 7, 16828−16836

Mesenchymal Vascular Cells: Pluripotency and Stemness Characteristics. *Cytotherapy* **2010**, *12*, 275−287.
(32) Wang, M.; Su, Y.; Sun, H.; Wang, T.; Yan, G.; Ran, X.; Wang, F.; Cheng, T.; Zou, Z. Induced Endothelial Differentiation of Cells from a Murine Embryonic Mesenchymal Cell Line C3H/10T1/2 by Angiogenic Factors in Vitro. *Differentiation* **2010**, *79*, 21−30.

DOI: 10.1021/acsami.5b04860
ACS Appl. Mater. Interfaces 2015, 7, 16828−16836